Copy
RM L52A15

NACA RM L52A15

NACA

RESEARCH MEMORANDUM

CHARACTERISTICS OF SWEPT WINGS AT HIGH SPEEDS

By Charles J. Donlan and Joseph Weil

Langley Aeronautical Laboratory
Langley Field, Va.

CLASSIFICATION CHANGED

To UNCLASSIFIED

By authority of Naca Res. abs. Date 2-8-57
+RN-112
AB 3-12-57

NATIONAL ADVISORY COMMITTEE
FOR AERONAUTICS

WASHINGTON
January 30, 1952

NATIONAL ADVISORY COMMITTEE FOR AERONAUTICS

RESEARCH MEMORANDUM

CHARACTERISTICS OF SWEPT WINGS AT HIGH SPEEDS

By Charles J. Donlan and Joseph Weil

INTRODUCTION

Progress is being made in subjecting to systematic study some of the many important factors affecting the behavior of swept wings at high speeds. In this paper are presented some of the results of recent swept-wing investigations that were undertaken to determine the effects of thickness and thickness distribution, camber and twist, nose-flap deflection, and devices or "fixes" for improving the wing pitching-moment characteristics at high lift coefficients.

SYMBOLS

C_L	lift coefficient
C_D	drag coefficient
$C_{D_{min}}$	minimum drag coefficient
C_m	pitching-moment coefficient
c_{l_i}	design section lift coefficient
L/D	lift-drag ratio
RN	Reynolds number
M	Mach number
$y_{c.p.}$	lateral center of pressure, percent semispan
b	wing span
c	wing chord
t	maximum wing thickness

α angle of attack

λ taper ratio

Λ sweep angle

$\Lambda_{c/4}$ sweep of quarter-chord line

Λ_{LE} sweep of leading edge

δ_n nose-flap deflection

EFFECT OF THICKNESS AND THICKNESS DISTRIBUTION

Lift-Curve Slopes

Wings of aspect ratio 3.5.- The lift-curve slope is a useful index for comparing different wings because it gives a direct indication of lift effectiveness and has an important influence on the drag due to lift for thin swept wings having little leading-edge suction. In figure 1 are shown the results of a study of the effects of thickness and thickness distribution on the lift-curve slope (average slope from 0 to $0.4C_L$) for various Mach numbers for a 47° sweptback wing of aspect ratio 3.5 and taper ratio 0.2. The data up to a Mach number of 1.15 were obtained in the Langley 8-foot high-speed tunnel (reference 1); the data at $M = 1.6$ were obtained with the same model in the Langley 4-foot supersonic pressure tunnel (unpublished). The fuselage was a cylindrical body with an ogival nose that was just large enough to house the strain-gage balance. Variations in uniform thickness ratio for these wings indicate only minor differences in the lift-curve slope and all wings possess regular although rapid variations in the transonic speed range. In the lower part of figure 1, a comparison has been made of the lift-curve slopes of a wing with a constant thickness ratio of 6 percent and one having a 6-percent-thick section over only the outboard 60 percent of the semispan. The root was thickened to 12 percent and tapered to 6 percent at the 40-percent semispan station. It is of interest that the tapered-in-thickness wing having a thickness ratio at the fuselage juncture of about 10 percent does not show any sudden losses in lift in this range. The theoretical variation of the lift-curve slope (references 2 to 4) has been added to indicate the confidence with which the data can be faired in the Mach number range for which data were unavailable.

Wings of aspect ratio 6.- An indication of the influence of aspect ratio on this thickness effect is afforded in figure 2. The data for the wing of aspect ratio 6 were obtained from bump tests in the Langley 7- by 10-foot high-speed tunnel. (See reference 5.) For this aspect ratio and sweep angle, it is apparent that a thickness ratio of 9 percent was not sufficient to avoid losses in lift in the transonic range, although the losses are nowhere near so severe as those encountered with the 12-percent-thick wing; however, it will be noted on the lower part of this chart that a tapered-in-thickness wing having a 9-percent-thick root section and a 3-percent-thick tip section was free of these losses and possessed characteristics similar to the constant 6-percent-thick wing. It appears, therefore, that some thickening at the root of a swept wing can be tolerated, provided the outer panel of the wing is thin enough.

It has been observed that the development of lift-slope "buckets" such as those shown for the 9- and 12-percent-thick wings occurs because of a breakdown in flow over the outer wing panel. Consequently, swept wings of high aspect ratio having this characteristic are likely also to have undesirable pitching-moment effects at low lift coefficients as illustrated in figure 3. These are the same wings for which lift-curve slopes are shown in figure 2. The wings exhibiting the very erratic pitching-moment behavior at $M = 1.0$ are seen to be the same wings that reveal a bucket-type lift-curve-slope variation in this range. The slopes of the curves of pitching moment against lift are plotted for different Mach numbers in the lower left part of the figure to provide an indication of the range over which this difficulty was experienced. The location of the lateral center of pressure is plotted against Mach number in the lower right part of figure 3. The inboard movement of the lateral center of pressure in the vicinity of Mach number 1 for the 9- and 12-percent-thick wings is evidence that the losses in lift are occurring over the outer panels of these wings. It will be noticed that this behavior did not occur on either the 6-percent-thick wing or the 9 to 3 percent tapered-in-thickness wing.

Effect of Sweep Angle.- The effects of thickness on the lift-curve slope are, of course, influenced by sweep angle as well as by aspect ratio. Although systematic data on this effect are scarce, some idea of the interdependency of these factors can be obtained from figure 4. This figure furnishes a convenient guide for estimating those combinations of aspect ratio, thickness ratio, and sweep angle that are likely to provide a smooth variation in lift-curve slope through the transonic range. The preferred combinations of these factors are those falling in the cross-hatched regions below the lines of constant sweep angle. The boundary for the zero-sweep line is well established from experimental data but the boundary for 45° sweep is only qualitative. Attention is called to the fact that the streamwise thickness ratio constituting the abscissa of this chart may be the root-mean-square value for a wing that is tapered in thickness and plan form.

Minimum Drag

Wings of aspect ratio 6.- Data obtained from rocket-model investigations (reference 6 and unpublished) showing the effects of thickness and thickness distribution on minimum drag are presented in figure 5. All wings were of aspect ratio 6, taper ratio 0.6, and were tested on a parabolic body. For purposes of comparison, the body drag has been subtracted and the minimum drag of the wing-fuselage combination less fuselage is presented. Although some mutual interference effects are undoubtedly present at Mach numbers close to 1, it is believed that at $M = 1.25$ these interference effects are small. Therefore, at this Mach number, the drag is cross-plotted against the square of the root-mean-square thickness ratio of these wings. It appears from this plot that the wings with the thickness modifications are probably contributing an amount of drag consistent with their weighted thickness.

Wings of aspect ratio 3.5.- Another thickness and thickness-distribution study has been completed at transonic speeds in the Langley 8-foot high-speed tunnel (reference 1) and the Langley 4-foot supersonic pressure tunnel (unpublished) and the results are presented in figure 6. These are the same wings for which lift-curve slopes were presented in figure 1. The wing-fuselage minus fuselage drag coefficients (WF-F) show the expected increases with thickness ratio. A cross plot of the data at Mach number 1.6 again demonstrates that the wing with the thickened root is contributing an amount of drag consistent with its weighted thickness. The reason for the delayed drag rise of the wing with the thickened root is not understood. It may be that, even with the small fuselage used on this model, favorable interference effects were encountered.

A study of the effect of sweep angle on the characteristics of the 4-percent wing of this family has also been made and the minimum drag results for the wing-fuselage less fuselage combination are given in figure 7. The results reflect the expected changes with sweep angle insofar as drag rise is concerned. Of some interest is the fact that the drag rise for this series of wings seems to have occurred at just about Mach number 1, as contrasted with the aspect-ratio-6 wings which showed generally increasing drag coefficients up to Mach number 1.4.

The calculated pressure-drag variation as determined from linear-theory charts (references 7 and 8) is shown for each of the swept wings. Even when adjusted to account for frictional effects as was done here, it is evident that these theoretical variations supply an inadequate guide for estimating the magnitude of the maximum drag rise that occurs at slightly supersonic Mach numbers.

Correlation of minimum-drag results.- Inasmuch as the excess of thrust over drag for a jet-powered airplane equipped with afterburning may be critical at Mach numbers just above 1, a knowledge of the drag in this region is especially important. It has been observed that a number of wings of aspect ratio 4 possess the characteristics exhibited by the wings of aspect ratio 3.5; that is, that the maximum pressure-drag rise occurs very close to $M = 1$. A correlation of this drag rise in the vicinity of $M = 1$ has been made for a number of wings of aspect ratio about 4 by using an empirical approach outlined in reference 9 and the results are shown in figure 8. The lines are those given by the empirical formula at the top of the chart where the thickness is taken in the stream direction. The points represent data from the indicated sources. That some orderly variation seems to exist for the pressure-drag rise in the vicinity of $M = 1$ seems evident but whether such correlations can be extended to other aspect ratios or even to other sections must await further study.

Pitching-Moment Behavior

Innumerable low-speed investigations have demonstrated the instability occurring at high and even moderate lift coefficient for those combinations of sweep and aspect ratio that may otherwise be attractive from performance considerations. It may be of interest to examine the effects of Mach number on this pitching-moment behavior (fig. 9). The wings of aspect ratio 6 were tested on the transonic bump in the Langley high-speed 7- by 10-foot tunnel (reference 5) and both were tapered in thickness as indicated, although thickness distribution has been found to have little effect on the particular characteristics under discussion. The wings of aspect ratio 4 were investigated in the Langley 8-foot high-speed tunnel (reference 10). It is seen that the severity of the pitching-moment reversal is lessened and delayed to higher lift coefficients as the transonic range is negotiated. Of particular importance is the rearward movement of the aerodynamic center at transonic speeds which tends to minimize the importance of the pitching-moment changes that are eventually encountered at high lift coefficients. It would appear, therefore, that, as far as the pitching-moment behavior is concerned, the most critical speed regime for high-aspect-ratio swept wings is likely to be at high subsonic Mach numbers where the pitching-moment characteristics are similar to those encountered at low speeds. Of course, tail-on tests will be required before any such conclusion can be stated with certainty.

METHODS FOR IMPROVING PERFORMANCE AND STABILITY

Performance

Twist and camber.- The use of twist and camber has been explored as one method of improving both the stability and performance of swept wings. Some results of one investigation of this kind are shown in figure 10. This investigation was conducted in the 12-foot pressure tunnel at the Ames Laboratory at a Reynolds number of two million. (See reference 11.) Both wings were of identical plan form. One had an NACA 64A010 section perpendicular to the quarter-chord line, whereas the other had an NACA 64A810 section perpendicular to the quarter-chord line and was washed out at the tip as indicated. Insofar as any improvement in pitching-moment behavior is concerned, the cambered and twisted wing was not much better than the basic wing at $M = 0.85$ and at $M = 0.94$ it was worse. From this and other investigations, it appears that something more than camber and twist is needed to improve the high-speed pitching-moment behavior of swept wings at high lift coefficients. To a certain extent, however, the study of this problem is complicated because at low speeds those wings which possess a fairly large amount of camber and twist show large Reynolds number effects. For high-speed investigations, the Reynolds numbers have been relatively low. It is evident, however, that, at this Reynolds number at least, a substantial improvement in performance at $M = 0.85$ resulted from the use of camber and twist even though for this wing the beneficial effect had vanished at $M = 0.94$.

It has been possible to twist and camber wings for improved performance at supersonic speeds, although specific examples of this kind are admittedly few. Figure 11 presents the maximum lift-drag ratios obtained for three wings designed from lifting-surface considerations specifically for operation at supersonic speeds. The aspect-ratio-3 wing was tested on the transonic bump at a Reynolds number of about one million and was designed for a uniform pressure loading for a lift coefficient of 0.25 at a Mach number of 1.1 (reference 12). The aspect-ratio-3.5 wing was designed for a uniform loading at a lift coefficient of 0.25 at a Mach number of 1.53 and was tested in the Ames 6- by 6-foot supersonic tunnel at Reynolds numbers up to 3.5 million (reference 13). The arrow wing was tested in the Langley 9-inch supersonic tunnel and was designed for $c_{l_i} = 0.20$ at $M = 1.62$ (reference 14). For each of these twisted and cambered wings a comparison with the corresponding flat wing was available. It is evident that some improvement was obtained throughout the Mach number range, at least for the Reynolds numbers of the tests. In fact, the configurations with aspect ratio 3.5 and 2.6 represent the highest lift-drag ratios that have been obtained in their respective Mach number ranges for purely swept wings. The results for the aspect-ratio-3 wing are for wing-alone data and the values of the lift-drag ratio are merely indicative of what might be accomplished.

Nose flaps.- One convenient device for studying camber effects is the nose flap. Preliminary tests have been made to explore the use of nose flaps at transonic speeds and the results obtained with a small semispan model in the Langley high-speed 7- by 10-foot tunnel (unpublished) are shown in figure 12. The ratio $\frac{\left[(L/D)_{max}\right]_{\delta_n}}{\left[(L/D)_{max}\right]_{flat}}$ indicates that the advantages of nose droop alone essentially disappeared at $M = 0.975$; however, with 3.5° of washout, the beneficial effects of nose-flap deflection were apparent at the highest Mach number for which data were available.

Stability

Regardless of the improvements in performance that some of the modifications discussed may lead to, the problem of instability at high lift coefficients is still the one for which it is most difficult to find a successful solution. Inasmuch as the use of leading-edge slats has been found to be an unattractive method for overcoming pitching-moment difficulties at high speeds, a considerable amount of research is being devoted to other methods of improving the high-speed, high-lift stability characteristics of swept wings.

Fences and chord-extensions.- Most of the progress that has been made in improving the pitching-moment characteristics of swept wings so far is attributable to "fixes." Fences, for example, are known from low-speed investigations to result in considerable improvements in stability. More recently, chord-extensions have indicated considerable promise at low speeds. Some recent results have been obtained on the relative effects of fences and chord-extensions at high subsonic Mach numbers and the results of one such investigation are shown in figure 13. The investigation described in figure 13 was conducted on a sting-supported model in the Langley high-speed 7- by 10-foot tunnel at a Reynolds number of 3.8 million (unpublished). The particular chord-extensions used were determined from extensive low-speed investigations on this wing. It will be observed that at $M = 0.8$ the single fence was nearly as good as the chord-extension in improving the characteristics up to a lift coefficient of 0.8 but, at higher lift coefficients and especially at higher Mach numbers, the chord-extension was more effective. Data (fig. 14) for a very similar wing but with a 0.15c chord-extension were obtained at a Reynolds number of 6×10^6 in the Langley 16-foot transonic tunnel (unpublished). At $M = 0.8$, the improvement obtained with the chord-extension was remarkable and, although the benefits of the chord-extension were less at high Mach numbers, some improvement is still evident at a Mach number of 0.98.

Inasmuch as the nose-flap results discussed earlier showed performance gains, the effect of chord-extensions and fences was also investigated in the Langley high-speed 7- by 10-foot tunnel with nose flaps deflected on the sting-supported model described in figure 13. The results of the nose-flap study are shown in figure 15 and it will be observed that the model is the same as that described in figure 13, except for the 0.20c leading-edge flaps that were drooped 6°. A comparison of the pitching-moment data with that of figure 13 shows that the nose flaps in themselves are relatively ineffective in producing any improvements in stability but that some improvement was obtained with a chord-extension or a fence. In general, the chord-extension was more effective than the fence for the wing regardless of whether the nose was drooped or not.

The effect of the chord-extensions on the maximum lift-drag ratio of this model, both with and without nose droop, is shown in figure 16. Of particular interest is the fact that whereas the chord-extension on the flat wing decreased the $(L/D)_{max}$ at the higher Mach number for the flat wing, the chord-extension on the wing with nose flaps actually increased the $(L/D)_{max}$ throughout the Mach number range. Although these arrangements are not considered optimum, they do indicate one possibility for improving both the performance and stability of swept wings. At the present state of our knowledge, these devices must be explored individually on each wing for which they are proposed.

RÉSUMÉ

In brief summary, data have been presented which indicate that:

1. Swept wings having appreciable taper in thickness appear to have characteristics similar to those which would be expected from a similar wing of constant thickness ratio equal to the root-mean-square thickness ratio of the tapered wing.

2. The maximum lift-drag ratios of sweptback wings can be improved by the judicious addition of camber and twist up to a Mach number of the order of 2.4.

3. The unstable pitching-moment variation developed by swept wings at high lift coefficients is characteristic throughout the subsonic and transonic Mach number range, although the severity of this effect appears to be somewhat diminished at transonic speeds partly as a result of the rearward movement of the aerodynamic center.

4. Arrangements of fences and chord-extensions can be developed on particular swept wings which materially improve the stability characteristics at high speeds without excessive loss in performance.

Langley Aeronautical Laboratory
National Advisory Committee for Aeronautics
Langley Field, Va.

REFERENCES

1. Bielat, Ralph P., Harrison, Daniel E., and Coppolino, Domenic A.: An Investigation at Transonic Speeds of the Effects of Thickness Ratio and of Thickened Root Sections on the Aerodynamic Characteristics of Wings with 47° Sweepback, Aspect Ratio 3.5, and Taper Ratio 0.2 in the Slotted Test Section of the Langley 8-Foot High-Speed Tunnel. NACA RM L51I04a, 1951.

2. Campbell, George S.: A Finite-Step Method for the Calculation of Span Loadings of Unusual Plan Forms. NACA RM L51L13, 1951.

3. Harmon, Sidney M., and Jeffreys, Isabella: Theoretical Lift and Damping in Roll of Thin Wings With Arbitrary Sweep and Taper at Supersonic Speeds. Supersonic Leading and Trailing Edges. NACA TN 2114, 1950.

4. Malvestuto, Frank S., Jr., and Hoover, Dorothy M.: Lift and Pitching Derivatives of Thin Sweptback Tapered Wings with Spanwise Tips and Subsonic Leading Edges at Supersonic Speeds. NACA TN 2294, 1951.

5. Morrison, William D., Jr., and Fournier, Paul G.: Effects of Spanwise Thickness Variation on the Aerodynamic Characteristics of 35° and 45° Sweptback Wings of Aspect Ratio 6. Transonic-Bump Method. NACA RM L51D19, 1951.

6. Pepper, William B.: The Effect on Zero-Lift Drag of an Indented Fuselage or a Thickened Wing-Root Modification to a 45° Sweptback Wing-Body Configuration as Determined by Flight Tests at Transonic Speed. NACA RM L51F15, 1951.

7. Margolis, Kenneth: Supersonic Wave Drag of Sweptback Tapered Wings at Zero Lift. NACA TN 1448, 1951.

8. Beane, Beverly: The Characteristics of Supersonic Wings Having Biconvex Sections. Jour. Aero. Sci., vol. 18, no. 1, Jan. 1951, pp. 7-20.

9. Polhamus, Edward C.: Summary of Results Obtained by Transonic-Bump Method on Effects of Plan Form and Thickness on Lift and Drag Characteristics of Wings at Transonic Speeds. NACA RM L51H30, 1951.

10. Wood, Raymond B., and Fleming, Frank F.: A Transonic-Wing Investigation in the 8-Foot High-Speed Tunnel at High Subsonic Mach Numbers and at a Mach number of 1.2. Wing-Fuselage Configuration Having a Wing of 60° Sweepback, Aspect Ratio 4, Taper Ratio 0.6 and NACA 65A006 Airfoil Section. NACA RM L50J25, 1951.

11. Johnson, Ben H., Jr., and Shibata, Harry H.: Characteristics throughout the Subsonic Speed Range of a Plane Wing and of a Cambered and Twisted Wing, Both Having 45° of Sweepback. NACA RM A51D27, 1951.

12. Spreemann, Kenneth P., and Alford, William J., Jr.: Investigation of the Effects of Twist and Camber on the Aerodynamic Characteristics of a Sweptback Wing of Aspect Ratio 2.98. Transonic-Bump Method. NACA RM L51C16, 1951.

13. Olson, Robert N., and Mead, Merrill H.: Aerodynamic Study of a Wing-Fuselage Combination Employing a Wing Swept Back 63°. - Effectiveness of an Elevon as a Longitudinal Control and the Effects of Camber and Twist on the Maximum Lift-Drag Ratio at Supersonic Speeds. NACA RM A50A31a, 1950.

14. Brown, Clinton E., and Hargrave, L. K.: Investigation of Minimum Drag and Maximum Lift-Drag Ratios of Several Wing-Body Combinations Including a Cambered Triangular Wing at Low Reynolds Number and at Supersonic Speeds. NACA RM L51E11, 1951.

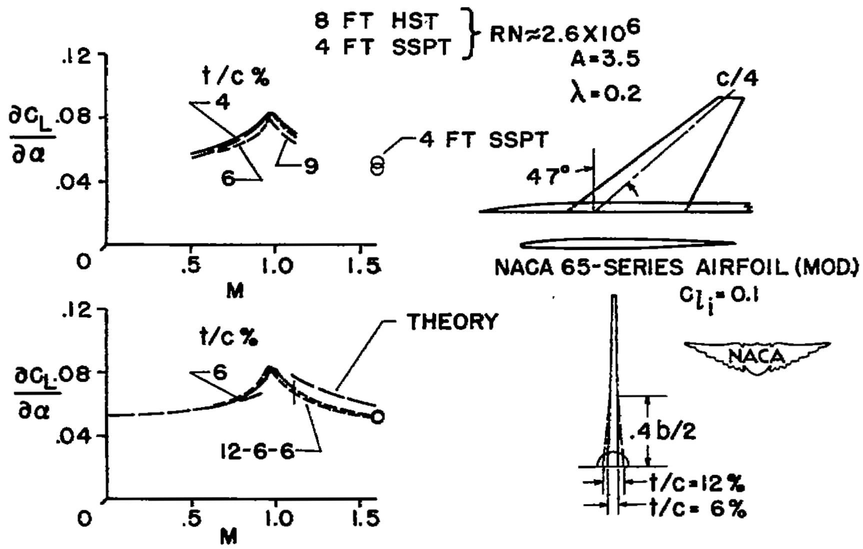

Figure 1.- Effect of thickness and thickness distribution on lift characteristics. A = 3.5.

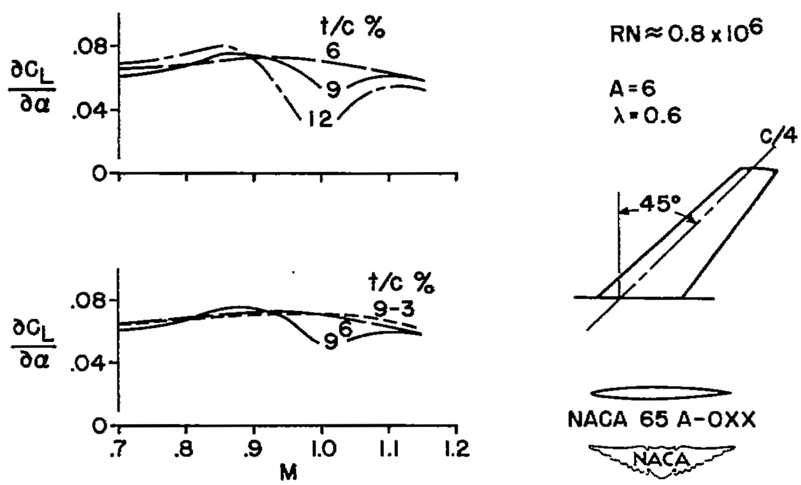

Figure 2.- Effect of thickness and thickness distribution on lift characteristics. A = 6.0.

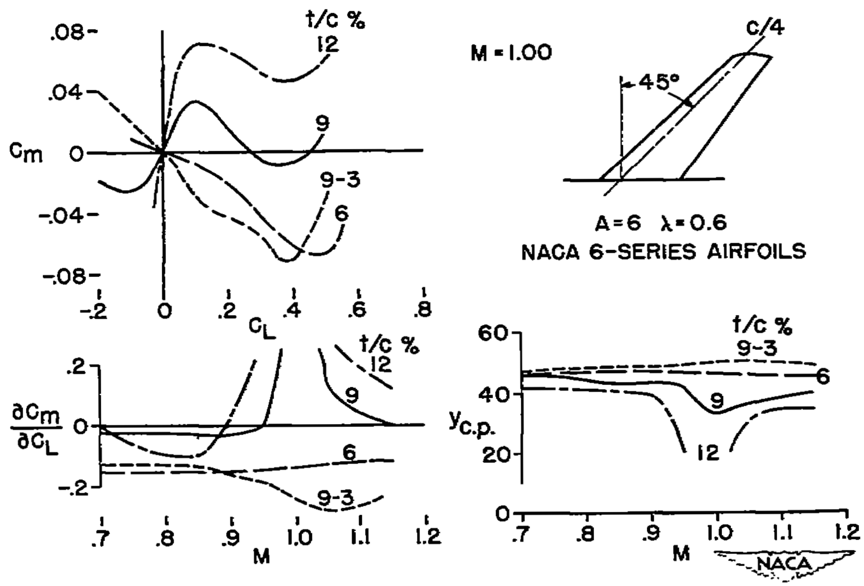

Figure 3.- Effect of thickness and thickness distribution on the pitching-moment and lateral center-of-lift characteristics. A = 6.0.

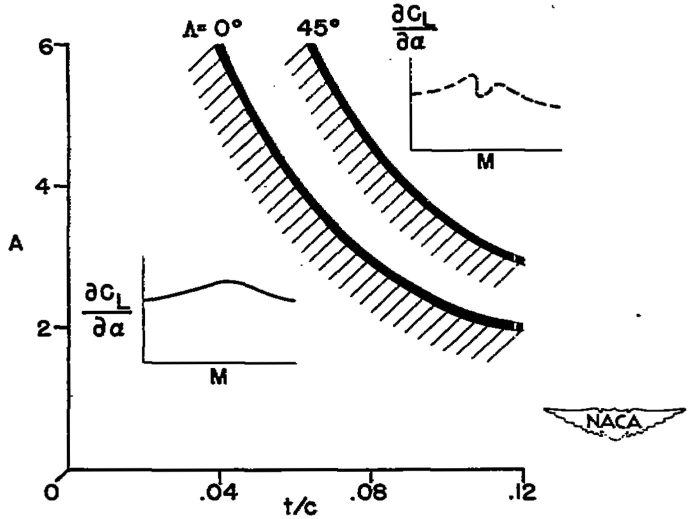

Figure 4.- Influence of aspect ratio, thickness ratio, and sweep angle on the type of transonic lift-slope variation.

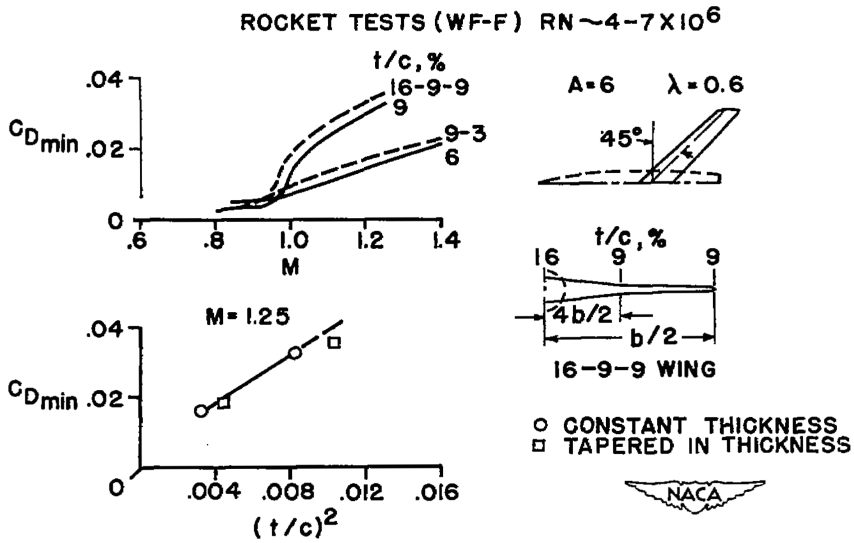

Figure 5.- Influence of thickness and thickness distribution on minimum drag. A = 6.

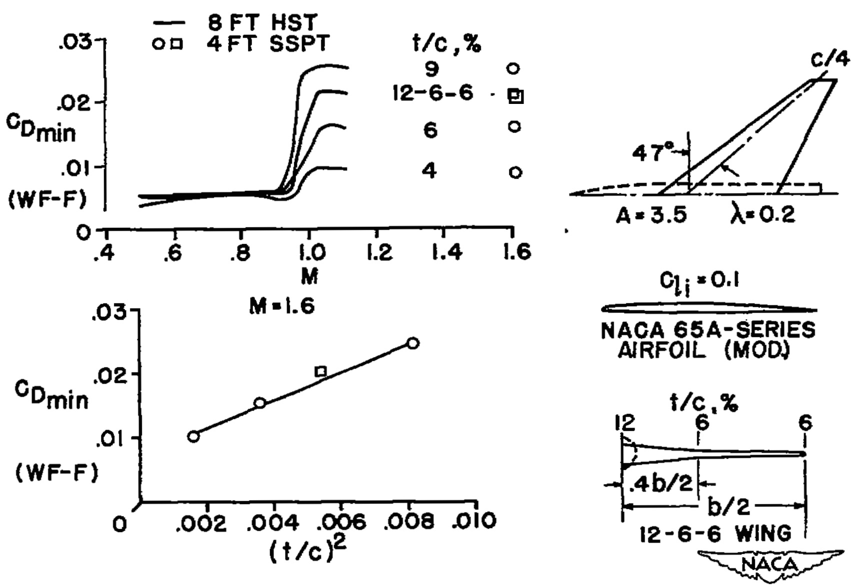

Figure 6.- Influence of thickness and thickness distribution on minimum drag. A = 3.5.

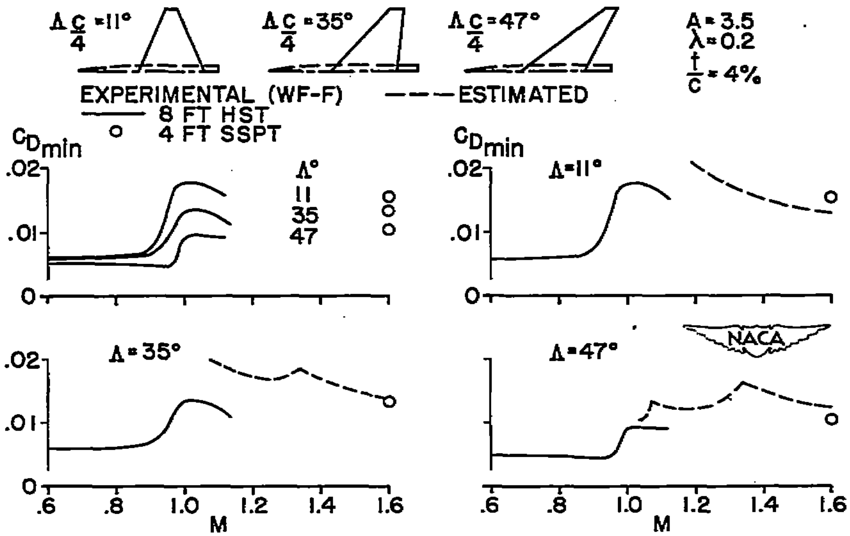

Figure 7.- Effects of sweep angle on minimum-drag characteristics. A = 3.5.

$$\Delta C_D = 2.83\left(\frac{t}{c}\right)^{\frac{5}{3}} \cos^{\frac{7}{3}} \Lambda_{\frac{c}{4}}$$

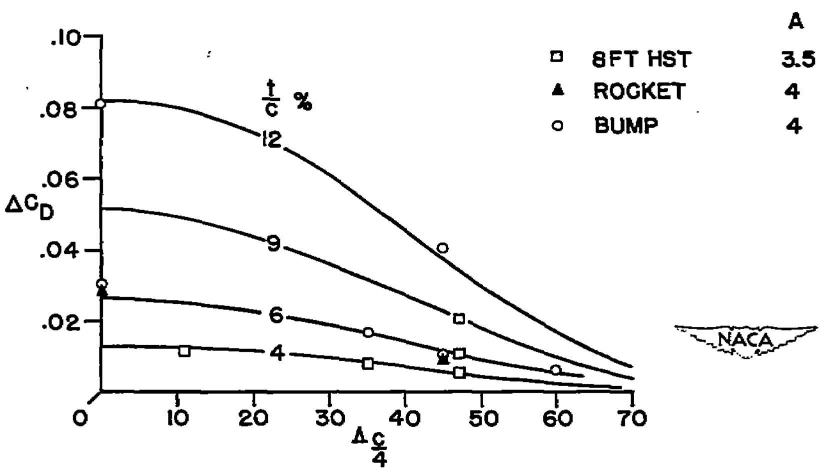

Figure 8.- Correlation of wave drag at low supersonic speeds.

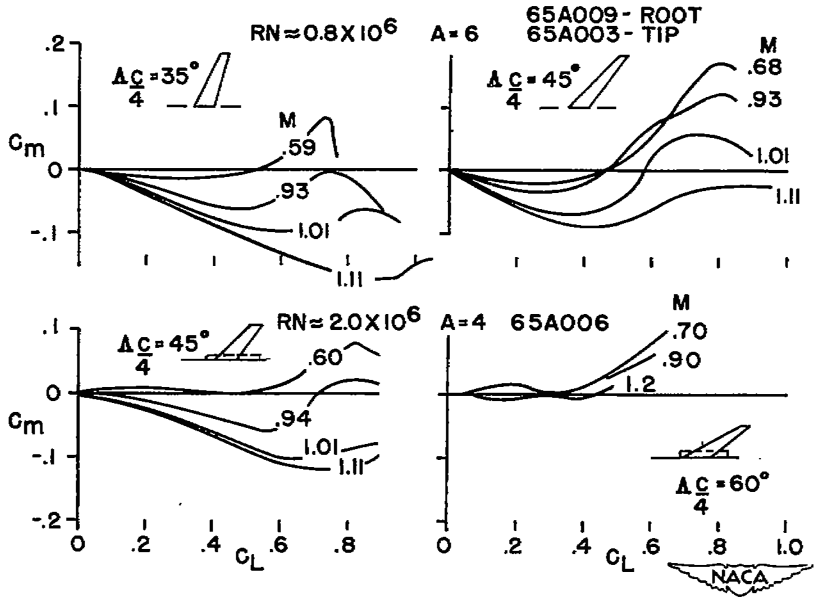

Figure 9.- Mach number effect on the pitching-moment characteristics of a number of swept wings.

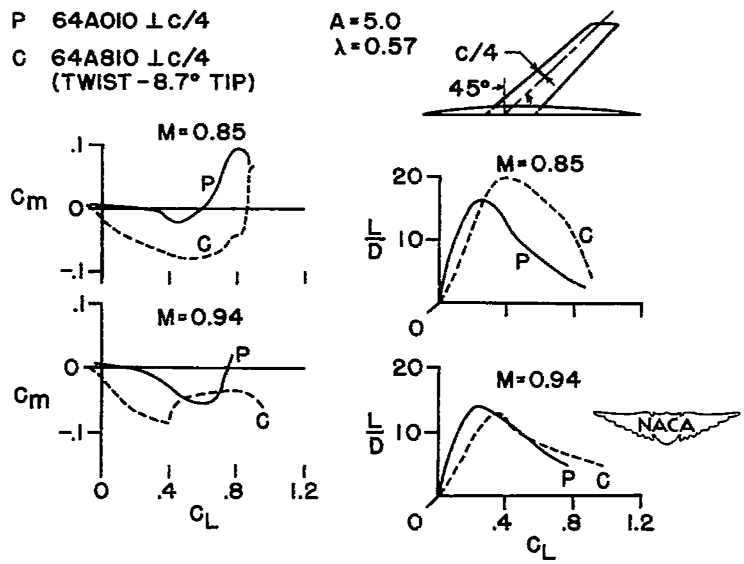

Figure 10.- Comparison of pitching moment and lift-drag ratios of a flat and a twisted and cambered wing.

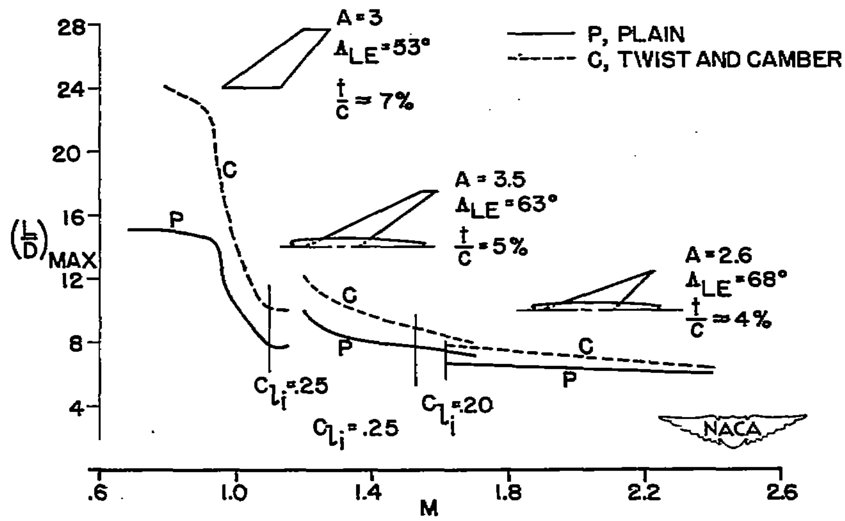

Figure 11.- Summary of effects of twist and camber on the performance of swept wings.

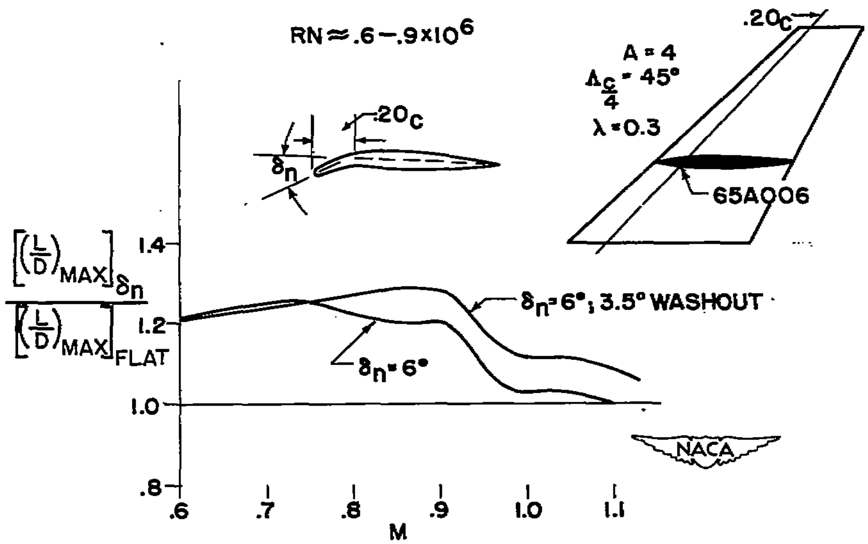

Figure 12.- Relative improvement in $(L/D)_{max}$ of flat wing attributable to nose-flap deflection.

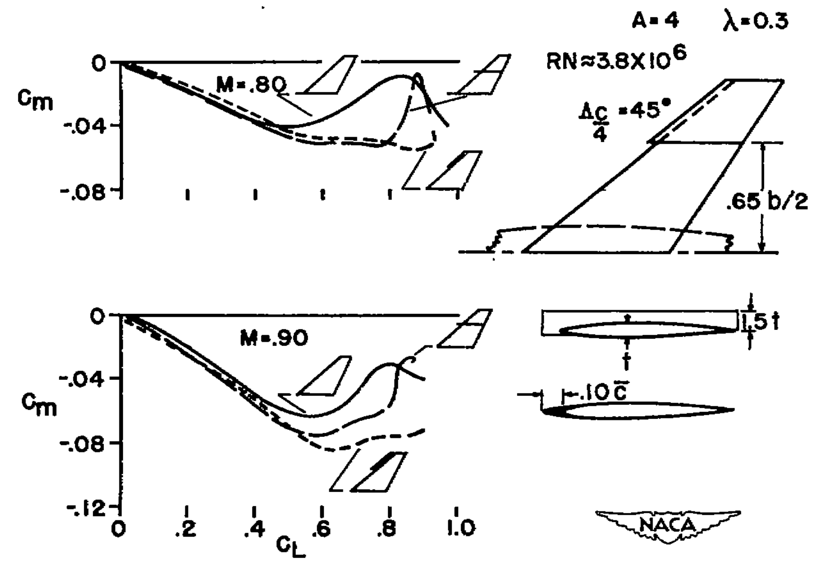

Figure 13.- Separate effects of chord-extensions and fences on the pitching-moment characteristics. RN = 3.8×10^6.

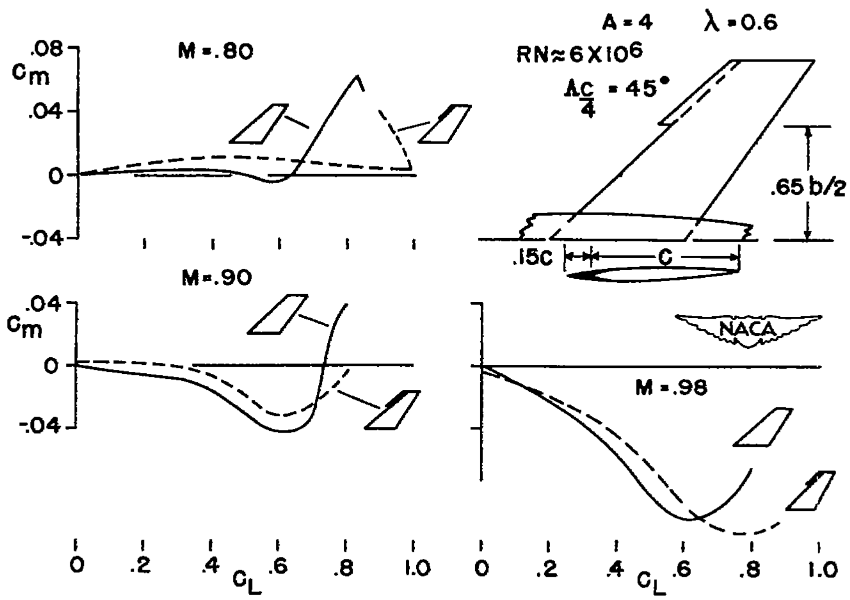

Figure 14.- Effect of chord-extensions on the pitching-moment characteristics of a swept wing at transonic speeds. RN = 6.0×10^6.

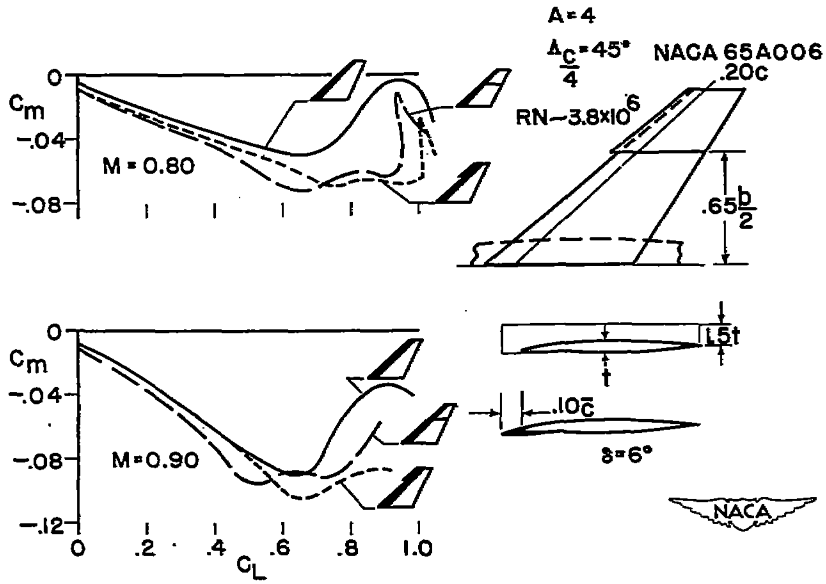

Figure 15.- Separate effects of chord-extensions and fences on the pitching-moment characteristics of a wing with nose flaps. RN = 3.8×10^6.

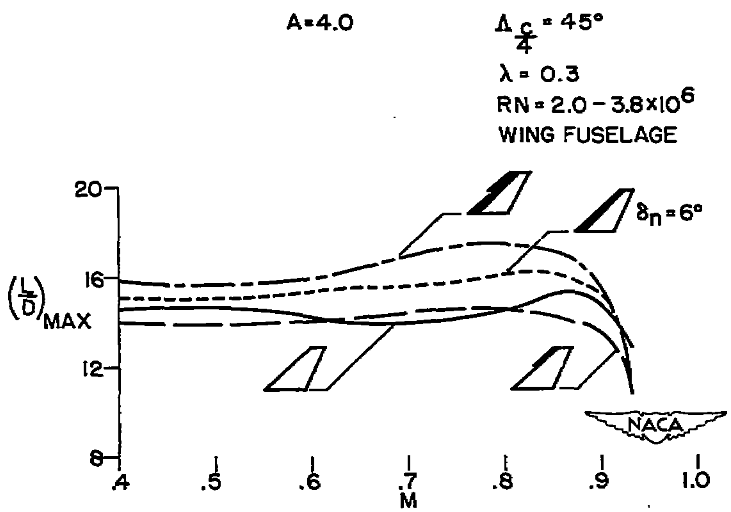

Figure 16.- Effects of chord-extensions and nose flaps on $(L/D)_{max}$.

NACA-Langley - 1-30-52 - 325

SECURITY INFORMATION

[redacted]

[redacted]